Research paper

Formation of zinc oxide particles in cetyltrimethylammonium-smectites

Nuttaporn Khumchoo [a], Nithima Khaorapapong [a,*], Makoto Ogawa [b,c]

[a] Materials Chemistry Research Center, Department of Chemistry and Center of Excellence for Innovation in Chemistry, Faculty of Science, Khon Kaen University, Khon Kaen 40002, Thailand
[b] Department of Earth Sciences and Graduate School of Creative Science and Engineering, Waseda University, Nishiwaseda 1-6-1, Shinjuku-ku, Tokyo 169-8050, Japan
[c] PTT Group Science and Technology Institute Project, 555 Vibhavadi Rangsit Road, Chatuchak, Bangkok 10900, Thailand

ARTICLE INFO

ABSTRACT

Zinc oxide was prepared in the interlayer space of cetyltrimethylammonium-smectites (a natural montmorillonite and a synthetic saponite) by the reaction between the aqueous solutions of zinc chloride and sodium hydroxide in the presence of cetyltrimethylammonium-smectites. The products were characterized by X-ray powder diffraction, Fourier transform infrared spectroscopy, as well as scanning electron, transmission electron, and optical microscopies. The formation of zinc oxide nanoparticles in the interlayer space of cetyltrimethylammonium-smectites was indicated by the transmission electron micrograph, diffuse reflectance absorption and the photoluminescence spectra. The photoluminescence of zinc oxide was affected by the interactions with cetyltrimethylammonium cation and silicate layer. The photoluminescence intensities of zinc oxide in cetyltrimethylammonium-saponite were higher than those in cetyltrimethylammonium-montmorillonite due to the quenching impurity in montmorillonite. Thus, the luminescence characteristics (both intensity and the energy) were controlled by the host–guest interactions with selection of host and modification.

© 2015 Elsevier B.V. All rights reserved.

1. Introduction

Functional semiconducting oxide nanoparticles have attracted increasing attention because of their unique properties and potential applications in optoelectronic, piezoelectricity, wide-band gap semiconductivity, photocatalysis, and so on (Zhang et al., 2000; Garcia et al., 2007; Comini and Sberveglieri, 2010; Yang et al., 2010; Al-Kahlout, 2012). Well-defined oxide-based nanoparticles with high surface-to-volume ratio, controlled surface defect, and designed shape and size are candidates for the applications, because the optical and electronic properties can be tuned by their morphology. Among available oxide semiconductor, zinc oxide (ZnO) is a wide band-gap semiconductor, which has been used for such application as pigment and photocatalyst for the decomposition of organic substance in waste water. Zinc oxide sometimes is a better photocatalyst than titanium dioxide (Xiong, 2010; Djurišić et al., 2012; Topkaya et al., 2014). Zinc oxides with controlled particle size and morphology have been prepared using complicated procedures, sophisticated equipments or environmentally unfriendly solvents (Garcia et al., 2007; Yadav and Pandey, 2009; Comini and Sberveglieri, 2010).

One of the alternative solutions to obtain a well-defined zinc oxide nanoparticle is controlling the growth and preventing their aggregation using the interactions with inorganic matrices. The hybridization of zinc oxide with silica (Sharma et al., 2009), mesoporous silica (Zhang et al., 2000; Chen et al., 2004; Jiang et al., 2006; Vaishnavi et al., 2008; Lu

et al., 2009; Mihai et al, 2010), and multi-walled carbon nanotubes (Chen et al., 2006; Zhu et al., 2009) has been reported so far. Among available inorganic solids for the immobilization of inorganic nanoparticles, layered materials are useful due to the expandable interlayer space and variable chemical nature of the layer surface. Taking advantages of such useful properties as swelling and ion exchange (van Olphen, 1977; Lagaly et al, 2006), smectite, a family of layered clay minerals, has received much attention as a scaffold to accommodate functional species to form hybrid materials. (Ogawa, 2004; Lagaly et al., 2006; Ogawa et al., 2014) A variety of hybrids of smectites embedding such nanoparticles of metal oxide (Németh et al., 2004; Hur et al., 2006; Kameshima et al., 2009; Xu et al., 2010), metal chalcogenides (Ogawa and Kuroda, 1995, 1997; Han et al., 2005; Khaorapapong and Ogawa, 2011; Okada and Ogawa, 2011; Ontam et al., 2011, 2012a, 2012b; Ruiz-Hitzky et al., 2011; Ide et al., 2013), metals (Malla et al., 1991) and metal complexes (Doner and Mortland, 1969; Pinnavaia and Mortland, 1971; Khaorapapong et al., 2011; Pimchan et al., 2011, 2014a, 2014b) with unique nanostructures and properties have been reported. Because the properties of the nanoparticle are defined by their size and morphology, attempts have been made to control the morphology of the embedded nanoparticles in or on the layered structure of smectites.

In this study, the formation of zinc oxide in the interlayer space of organically modified smectites, cetyltrimethylammonium montmorillonite and cetyltrimethylammonium saponite, was investigated. Organically modified layered solids have been used as building blocks of hybrids with various guests including ionically neutral and/or bulky species (Ogawa and Kuroda, 1995, 1997; Bisio et al., 2011; Okada and

Ogawa, 2011; Ruiz-Hitzky et al., 2011; Ide et al., 2013). Organically modified smectite is also useful for molecular recognition (Okada et al., 2012) and has been used to immobilize nanoscopic catalysts for photocatalytic application (Sasai et al., 2003, 2008, 2014). There are several papers on the interactions between inorganic nanoparticles and organically modified smectites, while, to the best of our knowledge, interaction of zinc oxide with organically modified smectites has not been reported. Here, two smectites were used because the negative charge densities on the silicate layers are different to lead different orientation of cetyltrimethylammonium cations in the interlayer space (Lagaly et al, 2006). The formation of zinc oxide in or on the inorganic solids including layered double hydroxide, sepiolite, magadiite and montmorillonite by ion exchange reaction and subsequent oxidation has been reported so far (Mogyorósi et al., 2001; Németh et al., 2004; Hur et al., 2006; Ozawa et al., 2009; Yuan et al., 2009; Xu et al., 2010; Fatimah et al., 2011). In the present study, attention is focused on the use of the organically modified montmorillonite and saponite for the controlled loading and states of the embedding zinc oxide particles. The location (on the inner and/or outer surfaces of cetyltrimethylammonium-smectites), the shape and the amounts of zinc oxide are possible parameters to obtain zinc oxide-smectite hybrids with varied optical properties.

2. Experimental

2.1. Materials

Two smectites including sodium-montmorillonite (Kunipia F, the reference clay mineral sample of the Clay Science Society of Japan, JCSS-3101) and sodium-saponite (Sumecton SA; the reference clay mineral sample of the Clay Science Society of Japan, JCSS-3501, synthesized hydrothermally by Kunimine Industries, Japan) were used as the host materials. The cation exchange capacities (CEC) of montmorillonite and saponite were 1.19 and 0.70 meq/g of clay mineral, respectively. Zinc chloride ($ZnCl_2$) and sodium hydroxide (NaOH) were supplied from Carlo Erba Regenti. Cetyltrimethylammonium (CTA, $C_{19}H_{42}BrN$) bromide (CTAB) was purchased from Sigma-Aldrich. All chemicals were used without further purification.

2.2. Sample preparation

Organically modified smectites (CTA^+Mt and CTA^+Sap) were prepared by conventional cation exchange reaction between the aqueous solution of CTAB and the aqueous dispersion of montmorillonite or saponite. The loading amount of CTA cation was adjusted just equal to the cation exchange capacity of the used montmorillonite and saponite (1.19 and 0.70 meq/g, respectively). After the cation exchange reaction, the zinc oxide (ZnO) precursors (aqueous solutions of zinc chloride and sodium hydroxide) were added into the dispersion of CTA^+Mt or CTA^+Sap and stirred vigorously at 70 °C for 24 h. The loading amount of Zn^{2+} was 1, 3 and 12 times of the CEC of the clay minerals. The colloidal stability of the samples was low in aqueous dispersion. Even after vigorous stirring, the solid precipitated within 15–20 min. Therefore, the resulting solids were easily separated by centrifugation. Then, the products were washed repeatedly with deionized water until a negative $AgNO_3$ test was obtained and dried at 40 °C for 3 days. The products were designated as $ZnO(n)CTA^+Mt$ and $ZnO(n)CTA^+Sap$, where "n" in the parenthesis indicated the loading amount (Zn^{2+}/CEC in equivalent) of ZnO in each sample.

2.3. Characterization

X-Ray powder diffraction (XRD) data were collected with monochromatic CuKα radiation using a Bruker D8 ADVANCE diffractometer. Thermogravimetric–Differential Thermal Analysis (TG–DTA) curves were recorded with a Perkin Elmer Pyris Diamond TG–DTA at a heating

rate of 10 °C min⁻¹ under a dry air flow using α-alumina (Al_2O_3) as the standard material. Fourier transform infrared (FT-IR) spectra were obtained with a Perkin–Elmer spectrum one FT-IR spectrometer using KBr disk technique. Scanning electron microscope (SEM) images were taken on a Hitachi S-2380 N scanning electron microscope. Transmission electron microscope (TEM) images were taken on a Tecnai G^2 20 LaB6 with an accelerating voltage of 200 kV. Diffuse reflectance UV–visible absorption spectra of the solid samples were obtained on a Shimadzu UV–VIS-NIR-3101PC spectrophotometer using an integrated sphere. Photoluminescence (PL) spectra were measured on a Shimadzu RF-5301PC spectrofluorophotometer in the wavelength range of 300–900 nm with the excitation wavelength of 350 nm. Photoluminescence quantum yields of the solid samples were determined on a Hamamatsu photonics C9920-02. Fluorospectroscopic photographs were taken on a Nikon ECLIPSE, E600 fluorescence microscope. N_2 adsorption–desorption isotherms were measured on a BELSORP mini instrument, BEL Japan, Inc., after the sample was degassed at 120 °C under vacuum for 3 h.

3. Results and discussion

3.1. Incorporation of ZnO in CTA^+Mt and CTA^+Sap

The XRD patterns of $ZnO(n)CTA^+Mt$ and $ZnO(n)CTA^+Sap$ are shown in Fig. 1, where a series of equally spaced reflections in the low angle regions were observed. The basal spacings of $ZnO(n)CTA^+Mt$ were ca. 2.0 nm and those of $ZnO(n)CTA^+Sap$ were ca. 1.5 nm. The expansion of the interlayer spaces was determined by subtracting the thickness of a silicate layer (ca. 1.0 nm) from the observed basal spacing to be ca. 1.0 and 0.5 nm for $ZnO(n)CTA^+Mt$ and $ZnO(n)CTA^+Sap$, respectively. No reflection due to ZnO crystal was seen in the XRD patterns of $ZnO(1)CTA^+Mt$, $ZnO(3)CTA^+Mt$, $ZnO(1)CTA^+Sap$, and $ZnO(3)CTA^+Sap$, indicating that the formation of bulk ZnO and/or the other species on the external surface of the silicate layers was suppressed or only a small amount of the ZnO crystal that could not be detected by the XRD technique existed on the surfaces. The XRD
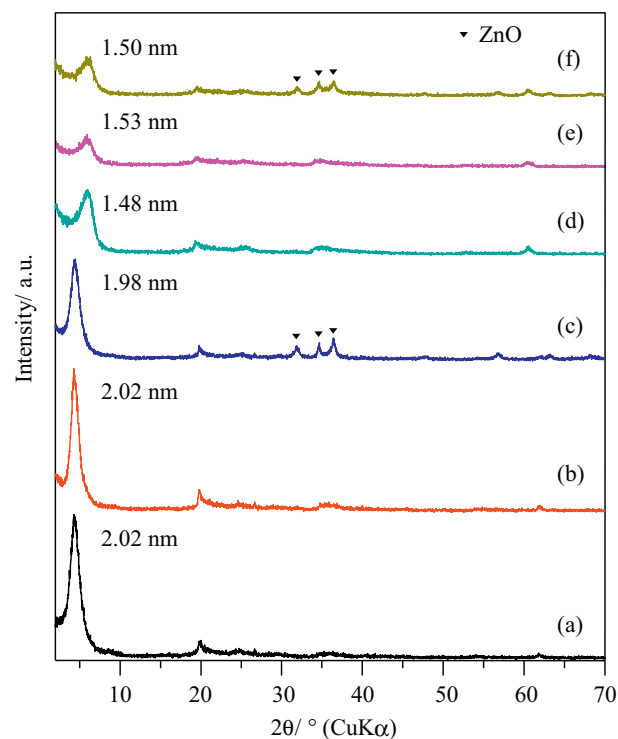

Fig. 1. XRD patterns of (a) $ZnO(1)CTA^+Mt$, (b) $ZnO(3)CTA^+Mt$, (c) $ZnO(12)CTA^+Mt$, (d) $ZnO(1)CTA^+Sap$, (e) $ZnO(3)CTA^+Sap$, and (f) $ZnO(12)CTA^+Sap$.